

Self-organized criticality in a bead pile

Rachel M. Costello, K. L. Cruz, Christie Egnatuk, D. T. Jacobs,* Matthew C. Krivos, Tim Sir Louis, Rebecca J. Urban,
and Hanna Wagner

Department of Physics, The College of Wooster, Wooster, Ohio 44691

(Received 12 September 2002; published 25 April 2003)

Self-organized criticality has been proposed to explain complex dynamical systems near their critical points. This experiment examined a monodisperse conical bead pile and how the distribution of avalanches is affected by the pattern of beads glued on a base, by the size or shape of the base, and by the height at which each bead was dropped onto the pile. By measuring the number of avalanches for a given size that occurred during the experiment, the resulting distribution could be compared to a power law description. When the beads were dropped from a small height, all data were consistent with a simple power law of exponent -1.5 , which is the mean-field model value. The data showed that neither the bead pattern on the base nor the base size or shape significantly affected the power law behavior. However, when the bead is dropped from different heights, then the power law description breaks down and a power law times an exponential is more appropriate. We found a scaling relationship in the distribution of avalanches for different heights and relate the data to an energy dissipation model. We both confirm self-organized criticality and observe deviations from it.

DOI: 10.1103/PhysRevE.67.041304

PACS number(s): 45.70.-n, 05.65.+b, 45.70.Ht

INTRODUCTION

Substantial effort has been devoted in recent years to understanding a new paradigm for complex, dynamical systems that are governed by short range interactions. After Bak, Tang, and Wiesenfeld (BTW) [1] proposed self-organized criticality (SOC) in 1987 as a way to explain phenomena as diverse as earthquakes, the stock market, forest fires, and ecology, some experiments and many simulations have been conducted. In SOC, a composite system whose many parts influence each other with short range forces would naturally evolve to a critical state where a small perturbation could lead to a minor or major event. The system would self-organize to a critical state without the need for a controlling parameter, such as temperature. The analogy of such a system being at its critical point and the implications for universal behavior were proposed by Bak and Tang [2] and further developed by others [3–6].

A system exhibiting SOC would have fluctuations on all length and time scales so that the distribution of events would follow a power law, perhaps with universal exponents, with many more small events than large ones and with most taking little time to complete. For example, the probability $P(s)$ of an event of size s would be given by the simple power law expression

$$P(s) = P_o s^{-\tau}, \quad (1)$$

where τ is the exponent. The system would not obey simple determinism in the sense that a major event could result from the same small perturbation as a small event. Moreover, there would be no way to predict when a major event would occur.

The original model system [1] for SOC was a sandpile. A bucket of dry sand turned upside down will form a conical

pile near the critical angle of repose. As more sand is sprinkled on the pile, avalanches of all sizes would form but the vast majority would be small in size and take place quickly. However, a few would deplete a significant portion of the pile. BTW [1] developed a cellular automata simulation of a sandpile with “toppling rules” that produced a power law behavior for the distributions of avalanche sizes and duration. Subsequent to their original article, many simulations and a few experiments have been conducted to test the robustness of SOC. Several reviews of granular systems have been written [7,8]. We will overview some of the more relevant work on the simple sandpile system.

PRIOR WORK AND THEORY

Experiments in avalanche dynamics in granular material have been in either “one-dimensional (1D)” piles, in slowly rotating cylindrical drums, or in conical piles. Altschuler *et al.* [9] studied the effect of the bead spacing on the base layer for a 1D pile confined between glass plates, which is a 2D geometry with flow in one dimension. When dropping 4-mm beads from 10 cm above the top of the pile, they found that the avalanche dynamics did not follow a power law in the size distribution, but did find a strong dependence on the base layer’s bead spacing. Christensen *et al.* [10] studied a rice pile in a similar 2D geometry and found SOC power law behavior for a region of avalanche sizes with an exponent τ of 2.4 ± 0.2 . Another study of rice in the same geometry [11] used the energy dissipated between successive profiles to measure the size of avalanches and found a dependence on the pile size (finite-size scaling) and the shape of the rice grains (aspect ratio). They found some shapes to follow a power law, while others did not. They also could describe their data with a stretched exponential of a form proposed by Feder [12] to explain other experimental data on avalanche distributions:

$$P(s) = P_o \exp[-(s/s_o)^\gamma], \quad (2)$$

*Author to whom correspondence should be addressed. Email address: djacobs@wooster.edu

where γ is the power that stretches the exponential to describe the data and s_o is the characteristic size. The presence of a characteristic size would be contrary to the system being at an SOC critical state. Others [13] also developed simulations to explain various aspects of the rice data.

Jaeger, Liu, and Nagel [14]; Evesque and co-workers [15]; and Morales-Gamboa *et al.* [16] have investigated granular material in a partially filled, cylindrical drum that would slowly rotate about the cylinder's axis. The resulting avalanches were not consistent with SOC predictions. A rotating drum advances a whole line of material past the angle of maximum stability and eventually takes more tightly packed material from the bottom of the pile and places it at the top, thus routinely rupturing force chains that support the grains [15]. It is this aspect that makes rotating drum experiments fundamentally different from the 2D geometry described above or the conical piles described below.

Held *et al.* [17] studied sieved "sand" in a conical pile supported by a digital mass balance. Aluminum oxide particles (average mass of 0.6 mg) were slowly added from 7.5 to 10 cm above the top of the pile and the mass of the pile was used to determine if avalanches occurred. By counting the number of avalanches that resulted in a particular mass loss off the edge of the pile, they found a power law of exponent 2.5 for sizes 3–80 grains with a characteristic decrease in the probability for avalanches which were larger. They also observed finite-size scaling in the distribution of avalanche sizes for the different diameter bases, which varied from 10 to 70 grain diameters.

Rosendahl, Vekic, and Kelley [18] conducted two experiments on conical piles that were similar to the Held *et al.* experiment: irregular grains dropped (from a small height of 0.5 cm in this work) onto a pile built on a mass balance that was used to measure the size of any avalanches off the edge. In their first experiment, they varied the diameter of the grains (0.4 and 0.8 mm) as well as the base diameter (25 to 100 grain diameters). They found a power law over the region of 2–20 grains that had a power of 2.2. In addition, they reported quasiperiodic large avalanches when the base diameter was larger than 75 grain diameters, an effect noted by Held *et al.* in the same regime. Their second paper investigated these large avalanches and proposed a scheme to predict major avalanches that might be useful in earthquake prediction. Others [19] have criticized their approach and the certainty with which one can make such a prediction.

Several years ago, our research group studied the robustness of avalanche dynamics when different types of beads were added to a conical pile. We measured [20] the mass of the pile after each bead addition and used the size of the avalanches off the edge of the pile to form the distribution, which was well described by a power law. Since the purpose of that investigation was to illustrate SOC, the small number of bead additions did not allow good statistics so that different functional forms could also describe the data.

Feder [12] proposed a stretched exponential [Eq. (2)] to describe selected data from all of the experiments done to that point. He found that a stretched exponential with γ between 0.34 and 0.44 would explain the data he analyzed. This value of γ is similar to the value 0.43 that Frette *et al.*

[11] found in rice piles. Since a characteristic size s_o was present in such a function, Feder [12] argued that SOC does not hold in granular systems. Furthermore, he notes that quasiperiodic avalanches are inconsistent with SOC.

In an effort to clarify the experimental situation for the simple sandpile model of SOC, we have carefully investigated a monodisperse, granular pile that is driven slowly by adding one grain at a time. We look at the size, shape, and packing of the base of the pile as well as the reproducibility for the avalanche distribution, something not mentioned in prior experimental work. Finite-size scaling, quasiperiodic large avalanches, predictability of major avalanches, and avalanche statistics were looked for and measured when observed. In addition, we systematically varied the height from which the beads were dropped onto the pile. As we will show, a simple power law describes the avalanche statistics if the beads are dropped from a small height, but a more complicated relation is needed when beads are dropped from a larger height. Moreover, the value we find for the exponent in the power law is much less than reported previously.

THEORY

The original work on SOC by BTW [1] was a paradigm shift in the approach to large, complex, interacting systems. By considering such a system as having organized itself to a critical point, then simple power laws should hold over a region when the system is near critical. Scaling relations have been developed as has the connection of SOC to a critical point [2–6], but most work in the field has relied on numerical simulations to investigate the phenomena for various systems. BTW proposed a sandpile as a model system for SOC; one that can be explored experimentally and numerically. However, experiments on sandpiles have shown a simple power law description for the avalanche distribution over only a fairly narrow region of avalanche sizes (one or two decades). Numerical simulations have either confirmed SOC or not, depending on the assumptions used; Cernak [21] reviews several numerical simulation results.

Several authors have developed a mean-field model for SOC using various approaches. In all of these, an avalanche is a front of noninteracting particles that can trigger additional activity or die out. This is a critical branching process [22] that typically involves tuning a parameter to reach the critical state. As Zapperi, Lauritsen, and Stanley [22] point out, this contradicts the assumption in SOC that the system is already at the critical point. They develop a mean-field model that avoids this paradox by using boundary conditions so that dynamics drive the system to the stationary state. The result [23] is a simple power law with an exponential cutoff,

$$P(s) = P_o s^{-\tau} \exp(-s/s_o). \quad (3)$$

The value of the exponent τ in the power law is 1.5, the same value others have found for mean-field models. The cutoff characteristic size s_o goes to infinity as the probability of a site relaxing (when stimulated by a neighboring site) goes to 1/2 [23]. This equal probability leads to the system being critical where the probability of an avalanche of size s is a simple power law.

The same equation is developed by Ghaffari, Lise, and Jensen [23] in a mean-field sandpile model that is nonconservative. Their model is a branched process where an “energy dissipation” moves the system from the critical point. In Eq. (3), they also obtain $\tau=1.5$ but the cutoff s_o depends on an energy dissipation parameter α as $1/s_o=(k-\alpha)^2$, where $(k-\alpha)$ approaches zero as the system approaches the critical point and is described by a simple power law. When a renormalization group analysis is done [23], then the dependence of the cutoff changes to

$$1/s_o \approx (k-\alpha)^{D_f/2}, \quad (4)$$

where D_f is the “fractal dimension of the avalanche” [23]. The concept of an energy dissipation that will take a system from the critical point is useful in our experiment. Vespignani *et al.* [24] argue that in the stationary state, the energy balance requires some critical exponents (including τ) to take their mean-field values in any spatial dimension as is observed in simulations [25].

EXPERIMENT

In an attempt to collect experimental data that can test the fundamental predictions of SOC, we use uniform, spherical glass beads to form a conical, granular pile as an idealization of a sandpile. The pile is formed on a base, which we vary in a number of ways, that is attached to a vertical support resting on a digital mass balance. We achieve a slowly driven system by adding one bead to the top of the pile and then waiting for a stable mass before the next bead is added. Avalanches are measured by the mass loss off the edge of the pile in the same way that Held *et al.* [17] and Rosendahl, Vekic, and Kelley [18] did. However, unlike these earlier studies, we use relatively large beads (3.0 ± 0.1 mm diameter, 0.035 ± 0.001 g) so we can then neglect wetting effects from room humidity that may cause cohesion in smaller beads [26].

The bead pile is built on top of a flat metal base where the first layer of beads are glued to prevent the pile from collapsing under its own weight. The pile is built by pouring 8000–40 000 beads onto the base and then a computer controlled bead dropper adds one bead at a time. The pile starts at its critical angle of repose, although occasionally there is a building period before major avalanches are detected. A LabVIEW program controls the experiment using a serial interface and collects the equilibrium mass of the pile as a function of time after each bead addition. A digital balance (Mettler PJ3000) measures the mass and has a resolution of 0.01 g, which allows us to measure individual bead additions and avalanches. The raw data are the mass of the pile and the time at which the mass is measured.

How the base is formed is reported to affect the distribution of avalanche sizes in 2D geometry piles [9]. We explored the effect of the base on the avalanche distribution in three ways. The first was the pattern by which the beads were glued to the base in a manner similar to that used by Alshuler *et al.* [9]. Using a 23 cm diameter base, three bead packings were constructed: one was close packed with no

space between beads, another used a fixed gap between beads measuring 1.25 bead diameters (center to center), while the third was a random packing that resulted from pouring beads onto the glue on the base. A second investigation explored the shape of the base on the avalanches using a 23 cm diameter circular base and a square base 23 cm on a side. The third set of experiments varied the diameter of the base from 13 to 28 cm in 5 cm steps. Held *et al.* [17] and Rosendahl, Vekic, and Kelly [18] reported both finite-size effects in similar experiments as well as a crossover to quasi-periodic large avalanches when the base diameter became larger than 70 bead diameters. The range of our base diameters covers a span from 40 to 93 bead diameters. While finite-size effects may be present, we will show in the following section that the distribution of avalanche sizes is not affected by any of these three modifications to the base. A simple power law with a universal exponent describes our avalanche size distributions well.

A fourth set of experiments varied the height from which beads were dropped onto the pile. The resulting kinetic energy of the dropped bead had to be dissipated in the pile and a systematic change in the avalanche size distribution was observed as the height increased. A deviation from a simple power law was observed with the occurrence of fewer large avalanches.

While these investigations have been done by different students over several years, many aspects have been consistent. First, the Mettler balance rests on a vibration isolation platform. For the suite of experiments investigating the effect of the base, an active isolation system (Newport optics table) was used. The experiments investigating the effect of the drop height were done with the balance on an optical bench (a passive isolation system). When the drop height is small, the avalanche distribution is independent of the isolation system used. In addition to the vibration isolation, all the experiments had a box over the pile and balance to eliminate drafts. We wanted to investigate the effect on the pile as a result of a bead addition and not from external vibrations.

The humidity where the granular pile formed was not actively controlled beyond the performance of the room ventilation system, which provides a relative humidity of 45% or less. Humidity effects have been observed when using small glass beads because of the surface wetting that can combine with glass dust to cause cohesive forces between the beads [27]. Glass dust forms from tumbling beads in a rotating drum or in recycled avalanche chutes, yet some would form from the type of piles and avalanches reported here. Such cohesive forces can cause aging in a pile—the pile becomes stronger and more resistant to shear forces in time. We have not seen this effect in our bead piles: whether fresh piles are created or the early versus later portions of a data run are analyzed on an established pile, we obtain the same avalanche distribution. This is a result of using larger (3 mm) beads, which are a factor of 10 larger in diameter and 10 000 in mass than the largest beads in which aging effects were observed from humidity-induced, cohesive forces [27].

In our slowly driven system, we always waited for avalanche activity to come to completion before recording a mass of the pile. Our balance updates the mass too infre-

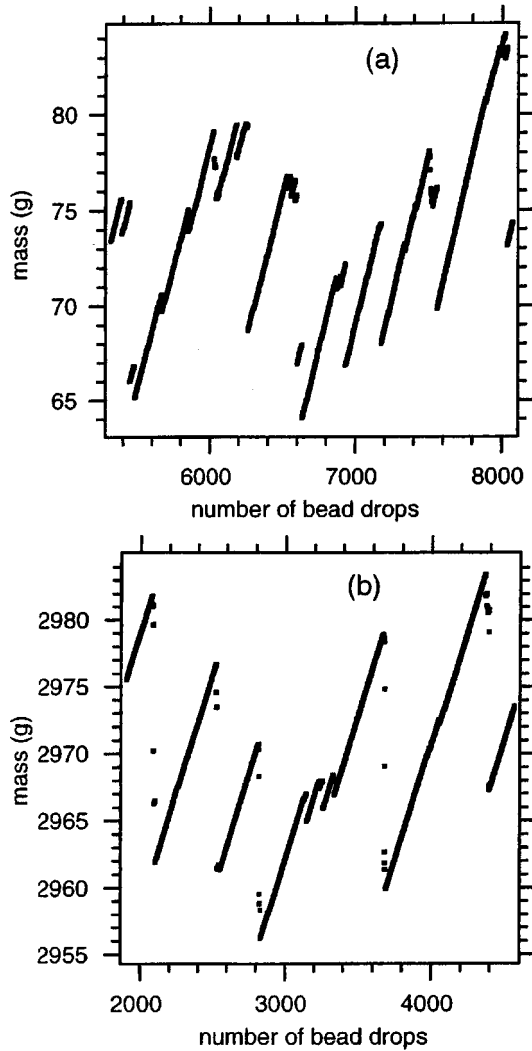


FIG. 1. The mass of the bead pile after each bead is dropped on the top of the conical pile shows periods of pile building interspersed with avalanches of all sizes. The “time” axis is the number of bead drops since the mass is recorded after the pile comes to equilibrium as a result of dropping a bead. Only part of each run is displayed with (a) from a pile with a 18 cm (60 bead diameters) base, while (b) is from a pile with an 28 cm (93 bead diameters) base. Neither shows quasiperiodic large avalanches.

quently to monitor an avalanche in progress, which usually takes less than a second to complete. However, larger avalanches sometimes take several seconds to finish. Our computer program waits for an equilibrium mass, which is at least 8 s for small avalanches and at least 30 s for larger ones. It is interesting that the largest drops in mass that are visible in the raw mass versus time data are almost always comprised of several smaller avalanches interspersed by periods of pile building.

A typical data run consists of building a pile on a base, then dropping one bead at a time while measuring the equilibrium mass of the pile. Subsequent data runs tested for reproducibility. From 15 000 to 50 000 beads were dropped onto the pile in runs that lasted from 54 to 95 h with 600 to 2000 avalanches occurring. Some piles were built fresh,

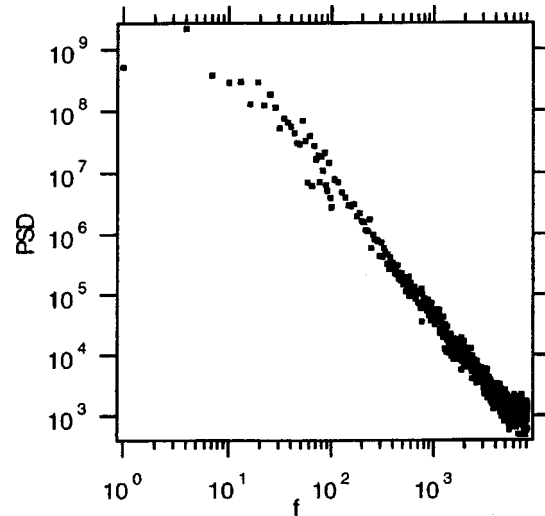


FIG. 2. The fluctuation in the mass for the 28 cm diameter base has a PSD that varies as a power law in “frequency.” The data fall on a line whose slope is ≈ -2 . The lack of a peak indicates a lack of quasiperiodic large avalanches.

while others were used from previous data runs. While we did not systematically investigate the packing of, and resulting force chains among, the beads on top of the base, we did not observe the appearance of the raw data nor the distribution of avalanche sizes to be affected by the pile history. While investigating the effect of the bases on the avalanche distribution, two data runs were typically used and averaged. When the height from which beads were dropped onto the pile was varied, three runs were taken with the same bead drop height. The data from the four drop heights were then used to estimate the error in our calculated probabilities, which we found to be typically 8%, but sometimes twice that for the larger, but far less frequent, avalanches. Similar error estimates have not been stated in other experimental work on the avalanche statistics of bead piles.

Before presenting the analysis of our data, it is interesting to look at the appearance of the raw data for two different pile sizes. Figure 1(a) shows a portion of the mass of an 18-cm base (60 bead diameters) pile as a function of time. A portion is shown since the data run is so long that the entire run will exhibit a digitization artifact when compressed for publication. The time axis is in bead drops since the time between bead drops varies. Large drops in mass correspond to large avalanches, but many small avalanches occur which cannot be observed at this scale. The mass on the vertical axis is not the total mass of the pile since only mass differences determine avalanches; thus, the balance was routinely tared when the pile was initially built, but before any data were collected. Figure 1(b) shows the same time portion as Fig. 1(a), but for our largest pile with a 28-cm base (93 bead diameters). The range of the vertical scale is larger for the larger pile, but the overall appearance is the same as in the smaller pile. In particular, the quasiperiodic large avalanche behavior, which others [17,18] have reported for bead piles with a base larger than 50–70 bead diameters, is absent in our data. In addition, large avalanches happened in our data without precursor events, thus preventing their prediction.

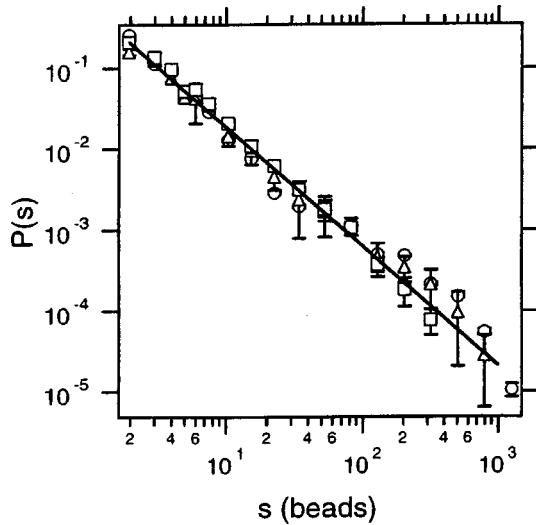


FIG. 3. The probability of an avalanche of size s as a function of the average avalanche size for that bin shows no dependence on the way in which beads were glued to the base. The circles are from an even gap spacing between beads, the triangles are close packed, and the square symbols are randomly packed. The line has a slope of -1.5 and indicates that a simple power law describes the data.

RESULTS AND ANALYSIS

From the raw data of the pile mass after each bead drop, one can easily obtain the change in mass, which corresponds to either a positive bead addition to the pile or to a negative mass change corresponding to an avalanche of beads off the edge of the pile. When comparing our results to theory, the size of the avalanche on the pile is assumed to be proportional to the size of the avalanche off the edge of the pile, which we can measure. Typically, the added bead stays on the pile, but an avalanche of any size can occur at any time.

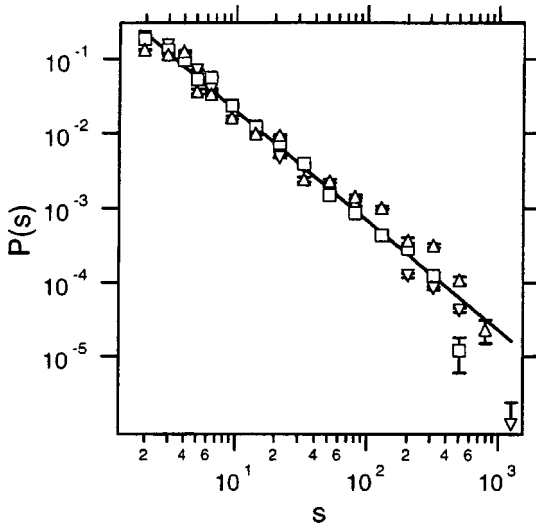


FIG. 4. The avalanche distribution does not depend of the shape of the base. The square symbols are from a square base 23 cm on a side, while the triangles are for circular bases 18 cm or 23 cm in diameter (∇ and Δ , respectively). The line guides the eye and has a slope of -1.5 .

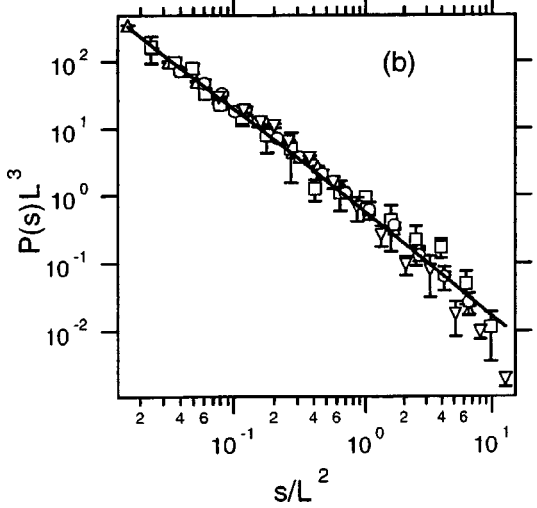
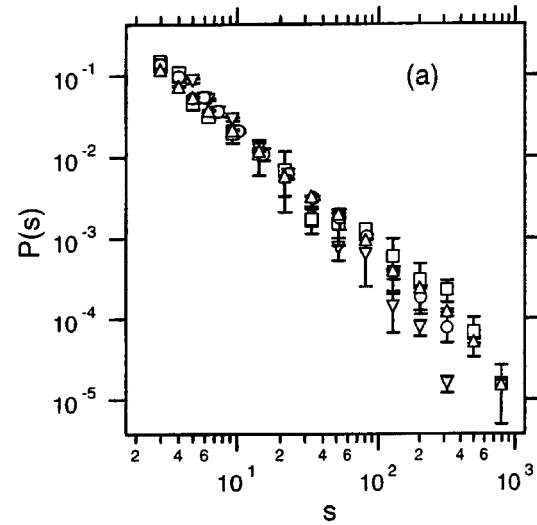


FIG. 5. When different diameter bases are used then the piles are different sizes but the avalanche distribution does not change significantly. For both plots, the ∇ are for 13 cm, the circles are 18 cm, squares are 23 cm, and Δ are 28 cm diameter base. Part (a) shows the avalanche distributions unscaled, while (b) shows the data on a scaled plot.

The lack of any characteristic time in the fluctuations of the mass of the pile is illustrated in Fig. 2 by taking the power spectral density (PSD) of the equilibrium mass of the 28-cm pile as a function of the number of bead drops (time) onto the pile. Since we cannot monitor the mass of the pile while avalanches are in progress, the resulting PSD reflects any periodicity in the equilibrium mass and not the time scale of the avalanches themselves. Figure 2 shows the PSD data as a function of “frequency” to approximate a power law decrease with an exponent of ≈ -2 . In particular, there is not a characteristic frequency that would indicate quasiperiodic large avalanches as observed [17,18] in piles even smaller than this one. The slope we observe is similar to the -1.92 ± 0.05 predicted from a lattice gas model [28] for a 2D geometry.

The raw mass of the pile is converted into a distribution of avalanche sizes by counting the number of avalanches within a size range or bin. Since the balance has a resolution

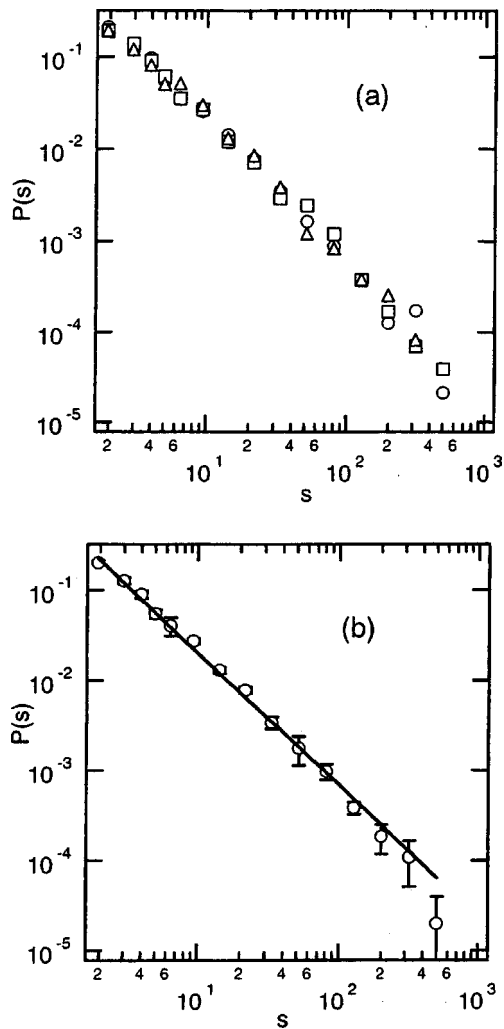


FIG. 6. The avalanche distribution when beads are dropped from 1.5 cm above the apex of a 18 cm diameter pile. In (a) the three data runs show the reproducibility, while (b) shows the average probability with its error. The line is a weighted fit to the data by a simple power law and has a slope of -1.47 ± 0.03 .

less than a single bead, we can measure small avalanches accurately. However, the smallest avalanche that can be detected is two beads falling off the pile, which is a result of adding one bead to the pile and observing a mass loss of one bead. Since there are so few large avalanches, binning of some kind is essential. The bin sizes are chosen to be evenly spaced on a logarithmic scale, but the precise choice of bin width does not change the shape of the distribution. The probability $P(s)$ for an avalanche of size s is the number of avalanches within the bin centered on s divided by the width of the bin and the total number of avalanches.

MODIFYING THE BASE

The packing of beads on the base has affected the avalanche character and distribution in 2D geometries [9], as has the shape and size [17,18] of the base. These earlier observations were tested in our research through three investigations. In the first investigation, three packing geometries

(close, fix gap, and random packing) were used on a 23 cm diameter base. Figure 3 shows that the resulting avalanche distributions for the three packings are consistent with each other and with a simple power law [Eq. (1)]. The line in the figure corresponds to an exponent τ of 1.5.

In the second investigation, the shape of the base was also varied. A square base 23 cm on a side was used as well as an 18 and 23 cm diameter circular bases. Figure 4 shows that the distribution of avalanche sizes are consistent with each other and with a simple power law of exponent $\tau=1.5$. These piles are evidently large enough that the avalanches along the surface do not know how the base is constructed. Even though the area of the bases is different, the avalanche distribution remains consistent as is shown in the following (third) investigation.

The size of the pile was varied by using circular bases of different diameters. We investigated piles whose base diameters were 13, 18, 23, and 28 cm, which correspond to 40–93 bead diameters. Indeed, the smaller piles did not have avalanches as large as the large piles. However, as shown in Fig. 5(a), all four sizes are consistent with a simple power law with exponent 1.5. A finite-size scaling analysis [29] can be done and is shown in Fig. 5(b), where $P(s) = L^{-\alpha} g(s/L^\nu)$. For the function g we use the power law given in Eq. (1), and L is the diameter of the pile. Since the average mass of the pile is constant, α and ν are related to τ by $\tau = \alpha/\nu$. Finite-size scaling does help align the smallest pile with the other sizes, but still with a simple power law description with $\tau = 1.5$. Since a systematic variation of the distribution with pile size outside its error bars was not observed, finite-size scaling does not make a significant difference.

The surprising result is that neither the base shape, packing, nor even size significantly affected the distribution of avalanche sizes. Moreover, a simple power law adequately describes all this data over three decades in avalanche size. The value of τ in the power law is the same for all the data: 1.5. This value is what mean-field theory predicts for the distribution of avalanche sizes. For these relatively large spherical beads, the size of the mass flow over the edge seems to be proportional to the size of the avalanche and to be well described by mean-field theory. This result is in sharp contrast to what has been observed in prior experiments where a simple power law would hold only over a narrow range of avalanche sizes and then with an exponent between 2.2 and 2.5.

VARYING THE DROP HEIGHT

The final set of experiments involved dropping the glass beads from different heights above the apex of the pile built on a 18-cm circular base. Four drop heights were used: 1.5 cm, 2.5 cm, 5.0 cm, and 10 cm. At each height, three data runs of 54 h each were collected, analyzed, and compared. One-fourth of the runs were on disturbed piles with the remainder on piles already at the critical angle of repose. Except for a building period for the disturbed piles, no difference in the avalanche statistics were observed which indicates that aging was not significant in the avalanche statistics for these piles. The three runs for the 1.5 cm drop

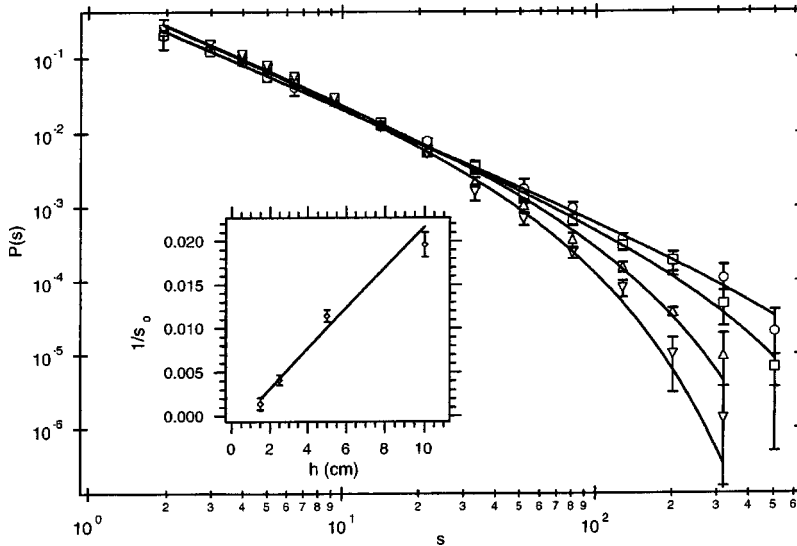


FIG. 7. The avalanche distribution systematically deviates from a power law as the height increases from which beads are dropped onto the pile. The circles are the average avalanche probability for beads dropped from 1.5 cm, the squares from 2.5 cm, Δ from 5 cm, and ∇ from 10 cm. The lines are weighted fits to the data for each drop height using Eq. (3) when τ is fixed at 1.47. The resulting s_o values have a systematic dependence on h as shown in the inset. The equation to the line is $1/s_o = -(0.0015 \pm 0.0007) + (0.0023 \pm 0.0002) h$.

height is shown in Fig. 6(a) and illustrates the reproducibility in the experiment. At each drop height, the probability is then averaged and an error is assigned that represents the reproducibility. The resulting distribution for the 1.5 cm drop height is shown in Fig. 6(b) along with a weighted fit to the data by a simple power law function given by Eq. (1). The resulting exponent value and one standard deviation error estimate is $\tau = 1.47 \pm 0.03$, a value consistent with the mean-field theory prediction of 1.5 and with data presented in the preceding section.

As the drop height increases, then the avalanche distribution deviates from a simple power law in a systematic way. Figure 7 shows the average avalanche distributions for the four drop heights and Table I provides the probabilities and error for each avalanche size and drop height. As the drop height increases, then the probability of large avalanches decreases with no avalanches in the largest bin. The number of

avalanches of size around 100 beads is roughly constant, but many more small avalanches occur as the drop height increases. Thus, the probability for an approximate avalanche size of 100 decreases as the drop height increases. However, the probability of small avalanches remains consistent for about one decade in avalanche size for all the drop heights. The kinetic energy of the dropped bead triggers more small avalanches so that the system is unable to reach a state where very large avalanches occur.

The energy that is dissipated in the pile can be likened to the energy dissipation parameter introduced in numerical simulations by Ghaffari [23]. The energy dissipation will be assumed to be proportional to the energy with which the bead impacts the pile, which is also proportional to the drop height h . The mean-field prediction is Eq. (3), which can be used in a weighted fit to the data. Holding $\tau = 1.47$, the value found for the 1.5-cm data, the amplitude P_o , and the characteristic size s_o were free in the fit and s_o was found to vary systematically with drop height as would be expected. Figure 7 shows the fitted lines to each drop height with the inset in the figure showing the dependence of s_o on drop height h . A linear dependence of $1/s_o$ on h is consistent with the data and would indicate from Eq. (4) a fractal dimension D_f for the avalanches of 2, which is reasonable for avalanches on the surface of the pile. The intercept of $1/s_o$ versus h is effectively zero, which would correspond in Ghaffari's model [23] to the bead pile being at the critical point when beads are added with no kinetic energy.

To illustrate the consistency of the data and the analysis using the mean-field model which gave Eq. (3), all the drop height data can be scaled. If Eq. (3) describes the data and if $1/s_o$ is just proportional to the drop height h , then all the data will fall on a common curve if a scaled plot is done. The scaling is done to eliminate the h dependence in s_o and gives $P(s)h^{-1.47} = P_o(s h)^{-1.47} \exp(-\beta s h)$, where β is the slope of $1/s_o$ versus h . Figure 8 shows all the data from different drop heights falling on a common curve when scaled in this fashion. The line is a weighted fit to the data and gives $\beta = 0.0020 \pm 0.0001$, which is within the experimental error of the slope found in inset of Fig. 7.

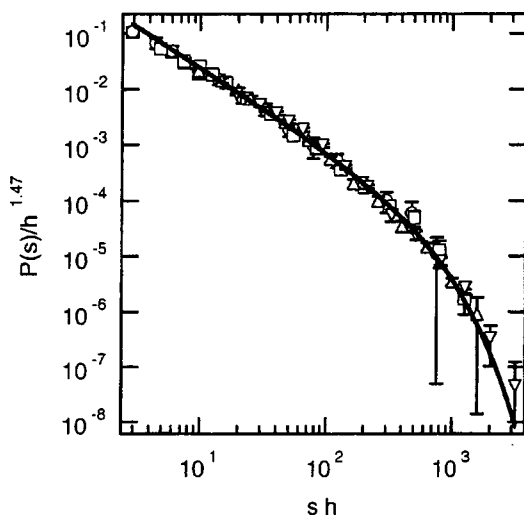


FIG. 8. All the avalanche distributions shown in Fig. 7 collapse onto a common curve when scaled. The symbols are the same as in Fig. 7. The line is a weighted fit to the scaled data using $P(s)h^{-1.47} = P_o(s h)^{-1.47} \exp(-\beta s h)$, where $P_o = 0.728 \pm 0.015$ and $\beta = 0.0020 \pm 0.0001$.

TABLE I. The probabilities P of having an avalanche of a size centered on s (in beads). Four different bead drop heights are presented (1.5 cm, 2.5 cm, 5.0 cm, and 10 cm). The error δP in the probabilities is from the typical standard deviation for avalanche probabilities in that size region. These data are plotted in Fig. 7. Numbers in square brackets denote powers of 10.

s (beads)	P ($s, 1.5$ cm)	δP (1.5)	P ($s, 2.5$ cm)	δP (2.5)	P ($s, 5$ cm)	δP (5)	P ($s, 10$ cm)	δP (10)
1.9	2.00 [-1]	1.1 [-2]	2.09 [-1]	8.7 [-3]	2.32 [-1]	1.0 [-2]	2.48 [-1]	1.0 [-2]
3.0	1.26 [-1]	1.1 [-2]	1.24 [-1]	9.5 [-3]	1.53 [-1]	1.5 [-2]	1.55 [-1]	1.2 [-2]
4.0	9.00 [-2]	8.4 [-3]	9.98 [-2]	7.6 [-3]	1.04 [-1]	8.1 [-3]	1.13 [-1]	8.6 [-3]
5.0	5.55 [-2]	5.8 [-3]	7.07 [-2]	6.1 [-3]	7.32 [-2]	7.7 [-3]	7.96 [-2]	6.1 [-3]
6.4	4.07 [-2]	9.3 [-3]	5.04 [-2]	5.1 [-3]	5.38 [-2]	4.1 [-3]	5.65 [-2]	4.3 [-3]
9.3	2.75 [-2]	2.2 [-3]	2.69 [-2]	2.5 [-3]	2.81 [-2]	2.1 [-3]	2.91 [-2]	2.2 [-3]
14.2	1.31 [-2]	1.0 [-3]	1.39 [-2]	1.1 [-3]	1.32 [-2]	1.0 [-3]	1.21 [-2]	9.2 [-4]
21.5	7.85 [-3]	6.5 [-4]	5.70 [-3]	8.5 [-4]	6.01 [-3]	7.0 [-4]	5.30 [-3]	4.0 [-4]
33.2	3.43 [-3]	5.4 [-4]	3.50 [-3]	7.2 [-4]	2.18 [-3]	3.4 [-4]	1.61 [-3]	3.9 [-4]
51.7	1.75 [-3]	6.2 [-4]	1.39 [-3]	2.2 [-4]	1.06 [-3]	2.0 [-4]	7.05 [-4]	1.3 [-4]
80.9	9.65 [-4]	1.9 [-4]	6.76 [-4]	1.1 [-4]	3.71 [-4]	7.9 [-5]	2.39 [-4]	3.7 [-5]
128	3.81 [-4]	5.9 [-5]	3.04 [-4]	4.7 [-5]	1.56 [-4]	2.4 [-5]	8.0 [-5]	2.0 [-5]
202	1.84 [-4]	6.6 [-5]	1.90 [-4]	5.5 [-5]	3.77 [-5]	4.9 [-6]	1.00 [-5]	6.9 [-6]
318	1.09 [-4]	5.7 [-5]	4.9 [-5]	2.5 [-5]	9.7 [-6]	9.5 [-6]	1.3 [-6]	2.3 [-6]
504	2.0 [-5]	2.0 [-5]	6.7 [-6]	3.1 [-6]				

A stretched exponential [Eq. (2)] has been proposed by Feder [12] and used to describe selected experimental data on avalanche distributions. It was found that earlier data could be explained with a value of γ between 0.34 and 0.44. We attempted to fit both our 1.5-cm data (Fig. 5) and the scaled data (Fig. 8) with a stretched exponential [Eq. (2)]. Neither dataset could be adequately described using a value of γ in this range. The fit to the 1.5-cm data would not converge and the value of γ approached zero. When γ becomes small, the effective range for the exponential function also becomes small. Thus, while the size of the experimental avalanches varied from 2 to 500 beads, the range of the exponential function when γ is 0.2, for example, becomes only a factor of 3 (1.15–3.47). The effect of a small value of γ is to collapse the data into a point, which an exponential function can pass through by varying the other parameters. Since none of the parameters in Eq. (2) have any physical significance and hence no limitation on possible values, a stretched exponential could always be found that describes the kind of distribution data presented here.

Indeed, the scaled data shown in Fig. 8 could be fitted as well by Eq. (2) as by Eq. (3). The values of the parameters in the weighted fit to Eq. (2) were $\gamma = 0.186 \pm 0.010$, $(P_o h^{1.47}) = 12.2 \pm 6.3$, and $s_o = (5.0 \pm 4.8) \times 10^{-4}$, where the error bars are one standard deviation estimates from the fit and are large because of the strong coupling of the other parameters to the value of γ . Unlike the parameters in Eq. (1) or (3), we do not know of a physical interpretation for the parameter values that described our scaled data using the stretched exponential of Eq. (2).

CONCLUSION

Monodisperse glass beads dropped onto a conical pile display avalanches that are consistent with self-organized criticality. A simple power law describes the avalanche distribution for a wide range of pile sizes and base configurations. The base made no difference in the avalanche distribution

and suggests that the avalanches on the surface of the pile are well removed from the details of the base. The assumption that the size of avalanches off the edge of the pile are proportional to the size of avalanches on the pile is supported by the lack of a pile size dependence in the avalanche distribution [30]. The robustness of the power law description over three decades of avalanche sizes is the strongest experimental confirmation yet for SOC. Moreover, the value of the exponent τ is the same in all the data and is the value 1.5 predicted by mean-field theory.

The 3-mm beads used are sufficiently large that we can neglect cohesive forces that result from glass dust and humidity. Aging of piles and cohesive forces are the result of glass dust and humidity that cause larger angles of repose and could be responsible for the quasiperiodic large avalanches others have observed [17,18]. Sufficiently large volumes of water added to bead piles has caused clumping [31]. The lack of such effects in our piles implies negligible cohesive forces compared to gravity.

As more energy is added to the dropped bead, the avalanche distribution deviates from a simple power law. The energy dissipation in the pile seems to gradually drive the system from the critical point. The mean-field model predicts a combination of a power law and an exponential that describes the avalanche distributions as the bead drop height was varied and provides physical insight into the system. The characteristic size s_o in the exponential is expected to depend on how far the system is from critical with it approaching infinity at the critical point. We find s_o to vary as the reciprocal of the drop height, or equivalently, the kinetic energy of the bead. This simple model describes our drop height data well, but we have too few heights to determine the precise dependence (see inset in Fig. 7). We suspect that dropping a bead from any height begins to move a system from the critical point, but our data are equally compatible with a threshold drop height of about 1–2 cm before the system

moves from criticality. We also suspect that s_o will be a function of cohesive forces as well as the frictional forces resulting from surface features on the granular material. This may explain the different experimental observations in the literature. In particular, a smaller probability of larger avalanches could give a larger experimental slope as the value of τ .

ACKNOWLEDGMENTS

We are grateful to Monwhea Jeng for helpful conversations and for bringing certain papers to our attention. The research was supported in part by NASA Grant No. NAG8-1433 with some student summer support from NSF REU Grant No. DMR 9987850.

-
- [1] P. Bak, C. Tang, and K. Wiesenfeld, *Phys. Rev. A* **38**, 364 (1988).
- [2] C. Tang and P. Bak, *J. Stat. Phys.* **51**, 797 (1988).
- [3] L. P. Kadanoff, S. R. Nagel, L. Wu, and S. Zhou, *Phys. Rev. A* **39**, 6524 (1989).
- [4] Yi-Cheng Zhang, *Phys. Rev. Lett.* **63**, 470 (1989).
- [5] P. Alstrom, *Phys. Rev. A* **41**, 7049 (1990).
- [6] D. Sornette, A. Johansen, and I. Dornic, *J. Phys. I* **5**, 325 (1995).
- [7] P. Bak and K. Chen, *Sci. Am.* **264**, 46 (1991); P. Bak, *How Nature Works: The Science of Self-Organized Criticality* (Copernicus, New York, 1996).
- [8] H. M. Jaeger and S. R. Nagel, *Science* **255**, 1523 (1992); S. R. Nagel, *Rev. Mod. Phys.* **64**, 321 (1992); H. M. Jaeger, S. R. Nagel, and R. P. Behringer, *ibid.* **68**, 1259 (1996); L. P. Kadanoff, *ibid.* **71**, 435 (1999).
- [9] E. Altshuler, O. Ramos, C. Martinez, L. E. Flores, and C. Noda, *Phys. Rev. Lett.* **86**, 5490 (2001).
- [10] K. Christensen, A. Corral, V. Frette, J. Feder, and T. Jossang, *Phys. Rev. Lett.* **77**, 107 (1996).
- [11] V. Frette, K. Christensen, A. Malthe-Sorensen, J. Feder, T. Jossang, and P. Meakin, *Nature (London)* **379**, 49 (1996).
- [12] J. Feder, *Fractals* **3**, 431 (1995).
- [13] L. A. N. Amaral and K. B. Lauritsen, *Phys. Rev. E* **56**, 231 (1997); M. Bengrine, A. Benyoussef, A. El Kenz, M. Loulidi, and F. Mhirech, *Eur. Phys. J. B* **12**, 129 (1999); M. Markosova, *Prog. Theor. Phys. Suppl.* **139**, 489 (2000); A. Malthe-Sorensen, *Phys. Rev. E* **54**, 2261 (1996).
- [14] H. M. Jaeger, C. Liu, and S. R. Nagel, *Phys. Rev. Lett.* **62**, 40 (1989).
- [15] P. Evesque, *Phys. Rev. A* **43**, 2720 (1991); P. Evesque, D. Fargeix, P. Habib, M. P. Luong, and P. Porion, *Phys. Rev. E* **47**, 2326 (1993).
- [16] E. Morales-Gamboa, J. Lomnitz-Adler, V. Romero-Rochin, R. Chicharro-Serra, and R. Peralta-Fabi, *Phys. Rev. E* **47**, R2229 (1993).
- [17] G. A. Held, D. H. Solina, D. T. Keane, W. J. Haag, P. M. Horn, and G. Grinstein, *Phys. Rev. Lett.* **65**, 1120 (1990).
- [18] J. Rosendahl, M. Vekic, and J. Kelley, *Phys. Rev. E* **47**, 1401 (1993); J. Rosendahl, M. Vekic, and J. E. Rutledge, *Phys. Rev. Lett.* **73**, 537 (1994).
- [19] E. Morales, R. Peralta-Fabi, and V. Romero-Rochin, *Phys. Rev. E* **54**, 3488 (1996).
- [20] S. K. Grumbacher, K. M. McEwen, D. A. Halverson, D. T. Jacobs, and J. Lindner, *Am. J. Phys.* **61**, 329 (1993).
- [21] J. Cernak, *Phys. Rev. E* **65**, 046141 (2002).
- [22] S. Zapperi, K. B. Lauritsen, and H. E. Stanley, *Phys. Rev. Lett.* **75**, 4071 (1995).
- [23] P. Ghaffari, S. Lise, and H. J. Jensen, *Phys. Rev. E* **56**, 6702 (1997).
- [24] A. Vespignani, R. Dickman, M. A. Munoz, and S. Zapperi, *Phys. Rev. Lett.* **81**, 5676 (1998).
- [25] A. Chessa, E. Marinari, A. Vespignani, and S. Zapperi, *Phys. Rev. E* **57**, R6241 (1998).
- [26] R. Albert, I. Albert, D. Hornbaker, P. Schiffer, and A. Barabasi, *Phys. Rev. E* **56**, R6271 (1997).
- [27] F. Restagno, C. Ursini, H. Gayvallet, and E. Charlaix, *Phys. Rev. E* **66**, 021304 (2002).
- [28] A. Karolyi and J. Kertesz, *Phys. Rev. E* **57**, 852 (1998).
- [29] S. Lubeck, B. Tadic, K. D. Usadel, *Phys. Rev. E* **53**, 2182 (1996).
- [30] V. Buchholtz and T. Poschel, *J. Stat. Phys.* **84**, 1373 (1996).
- [31] A. Samadani and A. Kudrolli, *Phys. Rev. E* **64**, 051301 (2001).